Groundwater discharge to coastal streams – a significant pathway for nitrogen inputs to a hypertrophic Mediterranean coastal lagoon

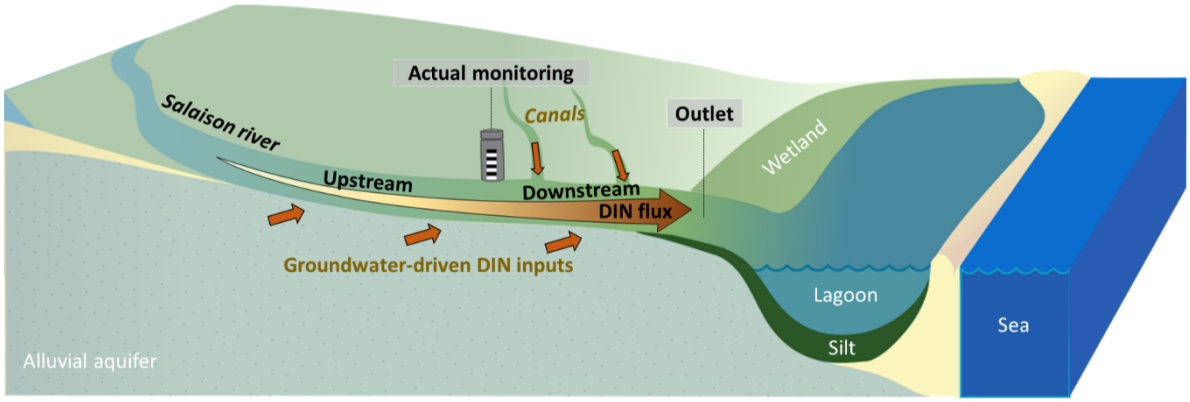
Marine **David**[1,2,3], Vincent **Bailly-Comte**[2], Dominique **Munaron**[1], Annie **Fiandrino**[1], Thomas C. **Stieglitz**[3,4]

1) Ifremer, UMR MARBEC (IRD, Ifremer, CNRS, Université de Montpellier, CNRS), Sète, France
2) NRE, BRGM, University of Montpellier,Montpellier,France
3) CEREGE, Aix-Marseille Université, CNRS, IRD, Coll France, 13545 Aix-en-Provence, France
4) Centre for Tropical Water and Aquatic Ecosystem Research, James Cook University, Townsville, Queensland 4811, Australia

Highlights

- Groundwater contribution to nitrogen fluxes was investigated in a major tributary to Or lagoon
- Groundwater is a major source of dissolved inorganic nitrogen (DIN) for the Salaison River
- DIN fluxes monitored at the Salaison gauging station are considerably underestimated
- Groundwater driven DIN inputs should be taken into account in coastal lagoons management actions

Graphical abstract



Abstract

Near-shore and direct groundwater inputs are frequently omitted from nutrient budgets of coastal lagoons. This study investigated groundwater-driven dissolved inorganic nitrogen (DIN) inputs from an alluvial aquifer to the hypertrophic Or lagoon, with a focus on the Salaison River. Piezometric contours revealed that the Salaison hydrogeological catchment is 42% bigger than the surface watershed and hydraulic gradients suggest significant groundwater discharge all along the stream. Hydrograph separation of the water flow at a gauging station located 3 km upstream from the Or lagoon combined with DIN historical data enabled to estimate that groundwater-driven DIN inputs account for 81-87% of the annual total DIN inputs to the stream upstream from the gauging station. A radon mass balance was performed for the hydrological cycle 2017-2018 to estimate groundwater inflow into this downstream part of the stream. Results showed that (1) DIN fluxes increased by a factor 1.1 to 2.3 between the gauging station and the Salaison outlet, (2) the increase in DIN was due to two groundwater-fed canals and to groundwater discharge along the stream, the latter represented 63-78% of the water flow. This study thus highlights the significance of groundwater driven DIN inputs into the Salaison River, which account for 90% of the annual DIN inputs. This is particularly true in the downstream part of the river, which, on averages, supplies 48% of total DIN inputs to the river. These DIN inputs into the Or lagoon were previously not taken into account in the management of this and other Mediterranean lagoons. The inputs will probably affect restoration processes for many years due to their residence time in the aquifer. This study throws light on a rarely documented source of 'very-nearshore' groundwater discharge to coastal streams in water and nutrient budgets of coastal zone ecosystems.

2. Introduction

Transitional water bodies like Mediterranean coastal lagoons are located at the interface between the continent and the sea, they are productive areas which provide substantial ecosystem services (Mooney et al., 2009; Newton et al., 2018). In these semi-enclosed water bodies, the gradient from fresh to saline water creates rich biodiversity which has been documented and protected for several decades now (Basset et al., 2013). As export to the open sea is limited, residence time in these water bodies is sufficiently long to enable assimilation of nutrients by living organisms (Kjerfve and Magill, 1989; Quintana et al., 1998). Coastal lagoons are thus particularly sensitive to nutrient fluxes resulting from anthropogenic activities (de Jonge et al., 2002; Newton et al., 2014). Excess nutrient inputs can lead to eutrophication of the water column, and proliferation of competitive species, thereby upsetting biodiversity equilibrium and reducing the quality of the water (Cloern 2001; Souchu et al. 2010). Among nutrient fluxes, the significant impacts of dissolved inorganic nitrogen (DIN) on eutrophication were already investigated three decades ago (Rimmelin et al., 1998; Taylor et al., 1995).

The main sources of DIN contamination investigated in the past are soil leaching from agricultural land, discharge from wastewater treatment plants (WWTPs), and urban and industrial effluents (Derolez et al., 2014). Indeed, DIN inputs from streams to coastal zones are mostly supplied by surface water, which transports agricultural inputs and wastewater (Meinesz et al., 2013). More recently, groundwater has also been considered as a source of DIN to the coastal zone (Johannes, 1980; Moore, 2010; Rodellas et al., 2015). These studies mainly focussed on direct submarine groundwater discharge (Burnett et al., 2006; Rodellas et al., 2018; Stieglitz et al., 2013) and some demonstrated that inputs from aquifers can significantly contribute to total coastal DIN inputs (Moore, 2010; Slomp and Van Cappellen, 2004). However, the contributions of groundwater inflow to streams discharging in the immediate coastal environment has rarely been investigated (Martinez et al., 2015; Peterson et al., 2010; Santos et al., 2010).

The goal of the present study was thus to assess inputs of DIN from a coastal aquifer system to a stream discharging into the hypertrophic Or lagoon located in the South of France. This lagoon suffers from recurrent eutrophication which led to a 'bad' ecological status according to the European Union Water Frame Directive (Symbo, 2017). Inputs of DIN from surface waters to the lagoon have been significantly reduced by management actions in the past 20 years, mainly thanks to improvements of wastewater treatment plants and to a lesser extent, to changes in agricultural fertilisation practices. However, despite these actions, no lasting improvement in the quality of the lagoon water has been observed (Derolez et al., 2017). As Salaison River is a perennial stream, groundwater inputs help maintain the water flow in periods with no rainfall, but the associated DIN fluxes have not previously been studied. Regional groundwater has high concentrations of DIN, and, given the comparatively long transit times and associated time lags before discharge, inputs from this coastal aquifer could be an obstacle to restoring Or lagoon.

Different methods are routinely implemented at different scales to study groundwater pathways to streams or to the coastline:

(1) At the aquifer scale, piezometric maps are used to identify drainage pathways, but this method requires a good knowledge of the aquifer geometry and its hydrodynamics properties (Burnett et al., 2001; Schilling and Wolter, 2007).
(2) At the surface watershed scale, hydrograph separation of streamflow data enables surface runoff to be distinguished from groundwater discharge (Chapman, 1999; Eckhardt, 2005; Schilling and Wolter, 2001). However, in coastal rivers, most gauging stations collecting such data are located a few kilometers upstream from the outlet to avoid the influence of the tide, which can lead to the underestimation of total inputs to the coastline (Santos et al., 2010).
(3) At a smaller scale, natural groundwater tracers like radon and radium are widely used to locate and quantify groundwater discharge into streams (Cook et al., 2003; Mullinger et al., 2007). High concentrations of these radionucleides are naturally found in groundwater whereas low concentrations are found in surface waters, making them efficient tracers of groundwater origin (Burnett and Dulaiova, 2003; Charette et al., 2001). Groundwater flow can be quantified using a mass balance along the stream (Cook et al., 2006; Peterson et al., 2010).

Even though combining approaches to improve our knowledge of the interactions between the aquifer and the coast would seems obvious (Burnett et al., 2001; Martinez et al., 2015), in the past, these methods were usually applied separately (Banks et al., 2011; Burnett et al., 2006; Menció et al., 2014). In the present study, the three approaches were combined to locate and quantify groundwater contribution to DIN inputs in Salaison River. In particular, groundwater inputs were investigated in the section of the stream close to the outlet, downstream from the Salaison gauging station. The three methods were combined to (i) obtain a more holistic view of the hydrogeological functioning of this coastal stream than is possible using a single method, (ii) estimate the groundwater contribution to the Or lagoon via the Salaison River, and (iii) assess more accurate DIN fluxes to the Or lagoon than estimated at the Salaison River gauging station.

3. Material and methods

3.1. Study sites

3.1.1. Or lagoon

The Or lagoon is located southeast of the city of Montpellier on the French Mediterranean coast (**Fig. 1a**). The surface area of the lagoon is 29.6 km² and the average depth is 1 m. In addition to the presence of an east-west salinity gradient, the lagoon is subject to marked interannual variations in salinity (from 2 to 35 psu). The northern bank of the lagoon is at the edge of 20 km² of wetlands which have been the subject of major land reclamations actions. The Or lagoon watershed covers 410 km², and has a flat landform rising from 0 (sea level) to 193 m asl (Blaise et al., 2008). The area is characterised by a typical Mediterranean climate. Precipitation is very low in summer, but intense rainfall events in spring and autumn can cause serious flooding. Annual average precipitation ranges from 600 mm in the southern part of the watershed to 750 mm in the northern part (Aquascop, 2013). The area is urbanized but agriculture still represents a major land use with intensively managed vineyards, market gardening, orchards and cereal crops. These activities have led to significant nutrient loading of the underlying aquifer, for

example, nitrate concentrations reach 1600 µmol.L^{-1} (i.e. 100 mg(NO_3)/L) in the eastern part of the aquifer (ADES database http://ades.eaufrance.fr).

The Or lagoon lies on a Holocene clay and clayey sand formation and is bound to the north by the coastal plain of Mauguio-Lunel (**Fig. 1a**). The adjacent Villafranchien aquifer is formed by the most recent layers of alluvial and colluvial deposits from the Pliocene and the Holocene, overlying a cretaceous and Jurassic limestone bedrock (Blaise et al., 2008). This aquifer outcrops over 252 km², it is limited to the west by the Lez River and to the east by the Vidourle River, and is partly fed by limestone (karst aquifer) along its north boundary. The aquifer is unconfined, except downstream at the edge of the lagoon where it becomes confined as it expands under Holocene silt. The presence of impermeable silt and clay from the Holocene prevents direct exchanges of water between the aquifer and the lagoon, but to date, little is known about the possible connections through the perennial streams which drain the aquifer (Blaise et al., 2008).

3.1.2. Salaison River

The Or lagoon is supplied with freshwater from natural streams and artificial canals (**Fig. 1a**). In the eastern watershed, the Lunel and Rhône to Sète canals bring water from the eastern alluvial plain. The present study focusses on the northern part of the watershed, where natural streams flow into the lagoon. Five main rivers and ten temporary streams flowing in a north-west south-east direction discharge into the Or lagoon. The Salaison River is one of the main tributaries flowing into the lagoon, which accounts for 59% (2015-2016) of the total freshwater supplied by the streams in the watershed (Colin et al., 2017). The Salaison River drains a 66 km^2 watershed which corresponds to 17% of the northern watershed of the Or lagoon. The source of the river is located on the northern Cretaceous limestone and, for its last nine kilometers, it flows over the Villafranchien aquifer.

The Salaison River used to receive effluents from four waste water treatment plants (WWTPs) (St Vincent de Barbeyrargues, St Aunes, Vendargues, Mauguio, with a total of 53 800 population equivalent) (Aquascop, 2013). In order to reduce inputs to Salaison and Or lagoon, St Vincent de Barbeyrargues WWTP (800 population equivalent) has not released any discharge into the Salaison since 2010, and the three other WWTP outlets were removed from the river between 2008 and 2011 (Symbo, 2014). Since then, diffuse surface and groundwater flows have been the sources of nitrogen inputs into the stream. In addition, the river is fed in its downstream part by two canals, one of which (Balaurie) used to receive effluent from the Vendargues WWTP (6 000 population equivalent) before it was removed and the other (Roubine) was used for urban and storm water drainage (**Fig. 1b**) .

3.2. Groundwater catchment of the Salaison river

A piezometric survey of the aquifer was carried out to identify the Salaison groundwater catchment, i.e. the area of the aquifer that interacts with the stream. Water levels were measured at 18 piezometers in high water table conditions on May 2nd and 3rd 2018 (**Fig. 1b**). Relative water level data were combined with the stream elevation and a digital elevation model to obtain the piezometric contours around the Salaison River by interpolation in ArcGIS.

Groundwater contours based on water table crests on both sides of the Salaison River were used to delineate the Salaison's groundwater catchment.

3.3. Salaison gauging station

Since 1986, stream water flow has been monitored through high-frequency limnimetric measurements made by the Regional Department for Environment, Development and Housing (French acronym DREAL). The gauging station is located 3 km upstream from the outlet to the lagoon and upstream from the Balaurie and Roubine canals (**Fig .1b**), capturing 75% of its total watershed (i.e. 50 km^2). Since 2006, DIN concentrations have been sampled by management agencies every two weeks under regular monitoring and at greater frequencies during floods, to assess DIN fluxes at the gauging station.

3.4. Combined methods upstream and downstream from the gauging station

In this study, two sections of the stream were distinguished based on the location of the gauging station: upstream and downstream sections. In the upstream section, the contributions of groundwater to the total DIN inputs at the gauging station were investigated. In the downstream section, additionnal inputs occuring between the gauging station and the Salaison outlet were also investigated, including the two downstream canals, along with groundwater contribution.

In any part of the stream, instantaneous DIN fluxes $f_X(t)$ (in $\mu mol.s^{-1}$) were estimated as the product of water flow $Q_X(t)$ (in $L.s^{-1}$) and DIN concentration $[N]_X(t)$ (in $\mu mol.L^{-1}$) (eq. 1) :

$$\boldsymbol{f_X(t) = Q_X(t).[N]_X(t)} \quad \textbf{(1)}$$

In the rest of the paper, the time increment '(t)' was removed for the purpose of clarity (i.e. f_X, Q_X and $[N]_X$).

First, total DIN fluxes were assessed in each section. Then, estimating groundwater driven DIN fluxes enabled to obtain the groundwater contribution to the total DIN fluxes. The two sections of the stream were approached differently (**Table 1**):

- the upstream part was investigated using historical data collected from 2013 to 2018 at the gauging station, to estimate total DIN fluxes $f_{station}$ and groundwater driven DIN flux f_{gw} (detailed in section **2.5**),
- Supplementary field data were collected in the hydrological cycle 2017-2018 for the downstream section, to estimate additional DIN fluxes $\Delta f_{downstream}$ and additional groundwater driven DIN fluxes Δf_{gw} using a radon mass balance (detailed in section **2.6**),

Instantaneous DIN fluxes f_X were integrated over one hydrological year (from September 1st to the following August 31st) and converted into tonnes to estimate annual DIN inputs F_X (in $tN.y^{-1}$). The relative groundwater contribution to the total DIN flux was estimated as the ratio of groundwater driven DIN flux to total DIN flux.

3.5. Groundwater contribution to DIN fluxes upstream from the Salaison gauging station

3.5.1. Water flow at the gauging station

Stream water flow data $Q_{station}$ at the gauging station (**Fig. 1b**) were extracted for the past five hydrological cycles from the DREAL database (hydro.eaufrance.fr, station Y3315080, 2013 - 2018) at hourly intervals, taking into account the fact that the Salaison has a fast hydrological response to rainfall (less than 6 hours between a rainfall event and an increase in flow).

3.5.2. DIN fluxes at the gauging station

Dissolved inorganic nitrogen (DIN) concentrations were extracted from the public water quality database Naïades (http://naiades.eaufrance.fr/). A total of 81 DIN data were collected from 2013 to 2018 and clustered according to their associated water flow to assess mean nutrient concentrations for three water flow classes $[N]_{station}$ (**Table 2**). The DIN flux at the gauging station $f_{station}$ is obtained using eq. 1 with $Q_{station}$ and the associated average DIN class concentrations $[N]_{station}$. Standard variations in DIN concentrations in each of the three classes were used to estimate uncertainty.

3.5.3. Groundwater flow at the gauging station

Groundwater flow Q_{gw} was obtained from hydrograph separation of the stream water flow $Q_{station}$. The Chapman model (Chapman, 1999) separates fast subsurface flow from base flow, the latter usually being driven by groundwater. The FlowScreen R package with the function bf_oneparam was used to assess time series of groundwater flow at an hourly time step. The recession constant was estimated for each hydrological cycle using the ESPERE tool (BRGM, Lanini et al. 2016), (μ= 0.971, σ= 0.019, n=5).

3.5.4. Groundwater end-member for DIN concentrations at the gauging station

Three sets of data were collected to determine the groundwater end-member for DIN concentration at the gauging station $[N]_{gw_s}$:

- piezometer P4 was sampled for groundwater DIN concentrations on March 8th, April 27th, May 5th, June 25th and July 27th in 2018. In this study, this well was assumed to be representative of the groundwater characteristics because of its location close to the gauging station (**Fig.1b**). In addition, piezometer St Aunes, located upstream of the Salaison watershed, was sampled on March 8th, June 25th and July 27th in 2018. For each sample, *in situ* salinity was measured using a multiparameter probe (WTW 3620).
- past DIN concentrations in groundwater at the P4 piezometer were taken from the BRGM study in 2006-2007 (Blaise et al., 2008). These past data were compared with new data to quamify changes in DIN concentrations over the past decade.
- stream data for DIN concentration and conductivity at the gauging station were also used to determine the groundwater end-member.

3.6. Groundwater contribution to DIN fluxes downstream from the Salaison gauging station

3.6.1. Water inflow downstream from the gauging station

3.6.1.1. Use of a radon and water balance to assess total and groundwater flow

A combined water and radon mass balance was constructed in the downstream part of the stream using two successive box models (**Fig. 2**) to estimate, for the hydrological cycle 2017-2018, (1) the additional groundwater discharge ΔQ_{gw} and (2) the total additional water flow $\Delta Q_{downstream}$ discharging between the gauging station and the outlet.

The first box for the radon mass balance includes the first 700 m downstream from the gauging station with the discharge from the Balaurie canal, and the second box, the section from 700 m to 2000 m, taking the discharge from the Roubine canal into account (**Fig. 1c**). The final section (2000 m-3000 m downstream from the gauging station) is affected by changes in lagoon water surface level caused by variations in wind and atmospheric pressure, as indicated by variable salinity. The last section can consequently not be considered as being in a steady state. Geological data showed that this section receives a negligible inflow of groundwater due to the impermeability of the underlying silt (**Fig. 1c**), it was not included in the model.

Data were collected when no rain had fallen in the two preceding days. In these dry hydrological conditions, surface runoff was assumed to be negligible in the mass balance and other than the two canals discharging into the boxes, no surface water inputs were taken into consideration. Since all field measurement were completed within a few hours, evaporation of stream water and precipitation were assumed to be negligible in the mass balance. In this case, only groundwater (ΔQ_{gw}) and canals (Q_{can}) composed the total water inflow downstream $\Delta Q_{downstream}$ (eq. 2) :

$$\Delta Q_{downstream} = \Delta Q_{gw} + Q_{can} \quad (2)$$

In these conditions, the stream was assumed to be in a steady state with respect to radon. Hyporheic fluxes were also included in the groundwater flow. The estimated groundwater discharge ΔQ_{gw} includes groundwater *sensu stricto* and hyporheic flux (Avery et al., 2018). The concentration of radon in a box was assumed to be the average concentration of radon in the inflow and the outflow (**Fig. 2**).

3.6.1.2. Radon sampling and analysis

Radon source and sinks used in the mass balance are summarised in **Table 3**. Next, we describe in detail the methods applied to measure radon concentrations in water, diffuse radon inputs from sediments, and atmospheric evasion.

Water was sampled once a month from January to July 2018 at five stations in the stream at 0, 50, 700, 750, 1 850 and 2 000 m downstream from the gauging station and in the two canals (**Fig. 1c**). Groundwater was sampled during the same period at piezometers P4 and St Aunes (same sampling as section 2.5.4). Water was sampled 20 cm below the surface using an immersed pump and primed directly into 2L bottles, thereby ensuring that the water sampled

did not exchange any gas with the atmosphere. Conductivity of the sampled water was measured with a WTW 3620 multiparameter probe.

Radon in the samples was analysed using an electronic Radon-in-air monitor (Rad7, Durridge Co.). ^{222}Rn was extracted from the water by continuous recirculation of air in a closed loop until it reached equilibrium. Equilibrium values in air were corrected to in-water values using standard methods (Burnett and Dulaiova, 2003; Stieglitz et al., 2013) (**Table 3**).

In order to determine diffuse inputs of radon, sediments were sampled from the bed of the Salaison River and incubated in a 2 L bottle filled with water (average dry weight: 11.92 g, σ=0.98, n=4) (Stieglitz et al., 2013). Samples were analysed with a Rad7 one month after being collected, when the sediments were assumed to be in equilibrium with the water, i.e. radon production equals radon loss by decay (Cook et al., 2008). The radon production rate can be estimated as follows (eq. 3):

$$Fdiff = Ceq.\lambda.\frac{Rinc}{Rfield} \quad (3)$$

where C_{eq} is the concentration of radon at equilibrium ($Bq.m^{-3}$), R_{inc} and R_{field} are the ratios of the volume of water to that of the sediment in the incubated sample and in the field, respectively. Average sediment depth was estimated at 0.4 m based on field observations. Average radon diffusion (F_{diff}) was calculated to be 600 ± 150 $Bq.m^{-2}.d^{-1}$ (n = 6).

Khadka et al. 2017 developed a method to assess atmospheric evasion at a known water temperature, density and velocity. Using this method in our study, atmospheric evasion (k) ranged between 1.6 10^{-5} to 2.5 10^{-5} $m.s^{-1}$ across the campaigns and was assumed to be constant in the stream for each campaign.

In each sampling campaign, water flow was gauged manually at the gauging station $Q_{station}$ and in the two canals Q_{can} as water flow inputs to the mass balance (**Table 3**). In addition, water flow at the Salaison outlet was gauged manually to validate the model outputs $\Delta Q_{downstream}$ with differential gauging.

To understand the link between groundwater inflow and groundwater dynamics and hydrological conditions, daily time series of water table fluctuation were obtained from the Saint Aunes piezometer on the ADES database (http://ades.eaufrance.fr / ID number BSS 09915X0181/AUNES), and annual rainfall data from the Meteo France database (Fréjorgues weather station).

3.6.2. DIN sampling and analysis downstream from the gauging station

At the same time as water was sampled for radon analysis, water was sampled to measure the concentration of DIN in the stream, the two canals and at piezometers P4 and St Aunes as described above in section 2.6.1.2 (**Fig 1c**).

Water samples were taken in HDPE 100 mL bottles, previously washed with analytical grade HCl 1.2N and rinsed with ultrapure water (UW) at the laboratory. All the sampling equipment and filters were rinsed with native water before sampling. Samples were filtered through a 100 µm filter for nitrate (NO_3), nitrite (NO_2), ammonium (NH_4), to prevent particles from interfering with the analysis of dissolved nutrients. Samples were immediately stored at -25°C

until analysis. The concentrations of the 3 forms of dissolved inorganic nitrogen were measured using SEAL AA3 Analytical Autoanalyzers using the method described in Aminot and Kerouel (2007) with colorimetric detection (from SEAL Analytical, Germany) and fluorimetric detection (from JASCO, FP-2020plus, France) respectively for, NO_2/NO_3 and NH_4. NID concentration was the sum of nitrites, nitrates and ammonium concentrations for each sample. Analytical grade standards KNO_3, $NaNO_2$, $(NH_4)_2SO_4$ were obtained from Sigma-Aldrich (St. Quentin Fallavier, France). Stock standard solutions were prepared in UW and stored in waterproof HDPE bottles at room temperature in the dark at the laboratory. Fresh working standards and calibration solutions were prepared daily by appropriate dilution of the stock solutions using gravimetric procedures. Laboratory quality controls (QC) were performed daily using gravimetric procedures and CertiPUR® NIST solutions (Merck, St-Quentin-en-Yvelines, France), to validate each analysis. The linearity of the calibration curves was always greater than $R^2 = 0.9996$. The limits of detection (LOD) were 0.05, 0.25 and 0.05 µmol.L^{-1} for respectively, NO_2, NO_3 and NH_4.

3.6.3. Estimation of annual DIN inputs downstream from the gauging station

The DIN flux at Salaison outlet was estimated as the sum of the DIN flux upstream and downstream, assuming negliglible in-stream nitrogen consumption (i.e. $f_{station} + \Delta f_{downstream}$). The increase factor ϕ_N between the DIN flux at the Salaison gauging station $f_{station}$ and the DIN flux at the outlet was estimated as follows (eq. 4):

$$\phi_N = \frac{f_{station} + \Delta f_{downstream}}{f_{station}} \quad (4)$$

Annual increase factor I_N was estimated for each hydrological year from 2013-2014 to 2017-2018 using the frequency of each water flow class in each hydrological year.

3.6.4. Groundwater driven DIN fluxes downstream from the gauging station

In the downstream part of the river, assuming negligible additional surface fluxes (2.3.1), DIN fluxes $\Delta f_{downstream}$ were assumed to be the sum of groundwater-driven DIN fluxes Δf_{gw} and canal DIN fluxes f_{can} (eq. 5):

$$\Delta f_{downstream} = \Delta f_{gw} + f_{can} \quad (5)$$

The relation between DIN and radon concentrations in the stream was used to determine the groundwater end-member downstream $[N]_{gw_d}$.

4. Results

4.1. Groundwater catchment of the Salaison River

The groundwater catchment i.e. the part of the aquifer connected to the Salaison River delineated by the piezometric crest on both sides of the river covers 32.9 km², which is 42% bigger than the Salaison watershed (i.e. surface water catchment) (**Fig. 3**). Piezometric contours show a main channel flowing from the north west to the south east of the aquifer underlying the stream, suggesting significant interactions between surface and groundwater. The contours suggest that on the most upstream part, water inflows from the stream to the aquifer, and downstream, the aquifer discharges into the stream. Along the last 4 km of the stream (i.e. where groundwater feeds the Salaison River), the hydraulic gradient decreases from 0.46 % upstream from the gauging station to 0.15 % downstream. Groundwater discharge may consequently be significant all along the downstream part of the Salaison River. Combined with the geological data, which revealed impermeable sediment units close to the lagoon, the decreasing hydraulic gradient showed that submarine discharge to the lagoon must be negligible, confirming previous conclusions.

4.2. Groundwater contribution to DIN fluxes upstream from the Salaison gauging station

Annual DIN inputs at the gauging station ($F_{station}$) ranged from 4.5 ± 1.8 $tN.y^{-1}$ for the dry hydrological cycle 2013-2014 to 55.2 ± 20.1 $tN.y^{-1}$ for the wet hydrological cycle 2014-2015 (**Fig. 4**), with 30.5 ± 11.1 $tN.y^{-1}$ for the hydrological cycle 2017-2018. DIN inputs were linked to annual precipitation (360 mm in 2013-2014; 1176 mm in 2014-2015). Nitrate (NO_3) was the main nitrogen form in the stream, with 74% to 99% of the total DIN concentrations.

In 2018, concentrations of DIN in the P4 well ranged around 600 $\mu mol.L^{-1}$ and reached higher values in the St Aunes piezometer (around 800 $\mu mol.L^{-1}$) (**Fig. 5**). Concentrations in the piezometer P4 remained in the same range in the three sampled years, suggesting that groundwater concentrations can be considered constant in the piezometer close to the Salaison River for the last five hydrological cycles. A correlation found between DIN concentrations at the station and specific conductivity (from DREAL) from 2013 to 2018, suggests that the DIN in the Salaison River originated from a high conductivity end-member (likely to be the 'theorical' groundwater end-member), diluted by mixing with a low DIN/ low conductivity end-member (**Fig. 5**). The latter end-member is likely to be surface runoff water since other DIN sources are negligible (section 2.1.2). Moreover, nitrate composed 95% to 100% of the total DIN forms in P4 and St Aunes and these proportions were similar in the stream. These results suggests that the highly enriched Villafranchien aquifer constitutes the main DIN source in the river.

In the upstream part of the Salaison River, the non-linear correlation between DIN concentrations and conductivity suggests that DIN in the stream cannot be the result of a conservative mixing between two end-members (**Fig. 5**). Based on high DIN concentrations / high conductivity measurements in the stream, the 'effective' groundwater end-member DIN concentrations are twice lower than DIN concentrations measured in the groundwater. The 'theoretical' groundwater end-member for DIN concentration is then reduced to the 'effective' groundwater end-member, suggesting nitrogen assimilation in the stream (i.e. from 600

392 µmol.L^{-1} to 300 µmol.L^{-1}). To estimate groundwater driven DIN inputs at the gauging station,
393 this 'effective groundwater' end-member was used, i.e. a DIN concentration of 300 ± 100
394 µmol.L^{-1} was assigned to $[N]_{gw_s}$.

395 The annual DIN flux from groundwater at the gauging station F_{gw} derived from hydrograph
396 separation Q_{gw} and 'effective' groundwater concentration $[N]_{gw_s}$ (in eq. 1) ranged from 3.9 ±
397 1.3 tN.y^{-1} (2013-2014) to 44.8 ± 14.9 tN.y^{-1} (2014-2015) (**Fig. 4**), with 25.9 ± 8.6 tN.y^{-1} for
398 2017-2018.

399 Annual groundwater contributions to instream DIN inputs ranged from 81% (2014-2015) to
400 87% (2013-2014), and 85% in 2017-2018. Contributions were lower for wet hydrological
401 cycles when surface runoff was more important, but annual groundwater contributions were
402 important as groundwater is a major DIN source in the stream. Thus, significant groundwater-
403 driven DIN fluxes are discharged upstream from the gauging station in this perennial stream.

404 ### 4.3. Interannual DIN fluxes downstream from the Salaison gauging station

405 #### 4.3.1. Interannual water inflow derived from the radon mass balance

406 Radon concentrations at piezometer P4 and St Aunes were sampled at maximum and minimum
407 table levels (from 14.5 to 16 masl at St Aunes), and ranged from 8 087 ± 178 to 12 412 ± 232
408 Bq.m^{-3} for P4 and 6 617 ± 327 Bq.m^{-3} to 8 580 ± 215 Bq.m^{-3} for St Aunes. Radon concentrations
409 were in the same range for the two piezometers, and radon concentrations at the P4 piezometers
410 were used as the end-member concentration in the radon mass balance for each campaign
411 (**Table 3**).

412 Radon concentrations in the stream at the gauging station ranged from 751 Bq.m^{-3} in January
413 to 1 378 Bq.m^{-3} in June, suggesting a considerable inflow of groundwater already occurring
414 upstream from the gauging station (**Fig. 6**). Importantly, radon concentrations increased
415 downstream from the gauging station, indicating significant groundwater influx. The increase
416 in radon concentration is evidence for direct groundwater discharge along the stream,
417 consistent with the geology in this section (**Fig. 3**).

418 Downstream water flow $\Delta Q_{downstream}$ estimated from the radon mass balance ranged from 55 ±
419 17 L.s^{-1} in July to 230 ± 73 L.s^{-1} in January (**Fig. 7**). At the Salaison outlet, confidence intervals
420 for water flow estimated with the radon mass balance overlapped those of manual gauging,
421 which enabled to validate the model outputs. Groundwater discharge estimated from the radon
422 mass balance downstream from the gauging station ΔQ_{gw} ranged from 43 ± 16 L.s^{-1} in July to
423 153 ± 53 L.s^{-1} in January, and contributed between 63% in April (high flows) and 78% in July
424 (low flows) to the total additional discharge $\Delta Q_{downstream}$. The radon mass balances were carried
425 out in different hydrological conditions (from 58 L.s^{-1} to 825 L.s^{-1} at the gauging station) but
426 the confidence interval remained in the same order of magnitude in most of the campaigns. The
427 absolute water flow discharging downstream, with significant uncertainties, did not seem to be
428 correlated (in a simple way) with the water table or with water flow at the gauging station
429 $Q_{station}$. Nevertheless, discharge downstream from the gauging station can have a significantly
430 impact on the water flow reaching the Salaison outlet, especially in dry conditions. For example
431 in July, downstream water discharge $\Delta Q_{downstream}$ increased water flow at the gauging station
432 $Q_{station}$ from 58 L.s^{-1} to 113 L.s^{-1} at the outlet.

4.3.1. Annual DIN inputs downstream

The relative increase in the DIN flux between the gauging station and the outlet ϕ_N was inversely correlated with the hydrological conditions (**Fig. 8**). When the water flow was low at the gauging station (dry conditions in July), the groundwater driven DIN flux downstream from the gauging station significantly increased the DIN flux at the Salaison outlet to a factor 2.3 ± 0.2. Conversely, in wet hydrological conditions (April), water flow at the outlet increased by a factor 1.1 ± 0.1. Absolute downstream DIN inputs remained in the same order of magnitude but, depending on the hydrological conditions, these inputs may have a significant influence on DIN flow at the outlet.

The annual increase factor I_N extrapolated from frequency-weighted water flow classes ranged from 1.8 ± 0.4 in 2014-2015 (in wet conditions) to 2.3 ± 0.6 in 2013-2014 (in dry conditions), and 1.9 ± 0.5 in 2017-2018. Annual DIN fluxes discharged directly into the downstream part of the Salaison River $\Delta F_{downstream}$ estimated with the annual increase factor I_N ranged from 5.6 ± 1.4 $tN.y^{-1}$ (2013-2014) and 43.1 ± 20.1 $tN.y^{-1}$ (2014-2015), and 28.1 ± 10.3 $tN.y^{-1}$ in 2017-2018.

4.3.2. Contribution of groundwater to the interannual DIN flux downstream

On the downstream part of Salaison River, the positive correlation between DIN and radon concentrations suggests that the DIN in the stream originated from the groundwater (**Fig. 9**). Maximum DIN values in the stream ranged between 300 and 400 $\mu mol.L^{-1}$, which was similar to the value used for the 'effective groundwater end-member' upstream ($[N]_{gw_s}$). With the similar end-member characteristics downstream (i.e. $[N]_{gw_d}$ = 300 ± 100 $\mu mol.L^{-1}$), the contribution of groundwater to the DIN flux downstream from the gauging station ranged from 56% in April (high flow) to 73% in July (low flows).

The concentration of radon in the Balaurie and Roubine canals (C_{can}) ranged from 2 298 to 7 664 $Bq.m^{-3}$, and their high radon and DIN concentrations were close to the values measured at the piezometers (**Fig. 9**). In addition, conductivity in the downstream part and the canals was high for all campaigns and reached the groundwater characteristics (**Fig. 6**). Since the field campaigns were conducted in dry periods, water discharging from these short canals probably only originate from groundwater and drain the lower aquifer units. Average flow in the Balaurie and Roubine canals remained between 20 $L.s^{-1}$ in dry hydrological conditions and 50 $L.s^{-1}$ in wet hydrological conditions. Consequently, canal discharge was counted as groundwater inflow, to be added to direct inflow to the main Salaison channel, meaning that groundwater contribution to total DIN flux in the downstream part was 100%.

4.4. Overall groundwater contribution to the inputs at Salaison outlet

At the Salaison outlet, the downstream inputs from groundwater and canals significantly increased the total DIN inputs reaching Or lagoon (i.e. $F_{station}+\Delta F_{downstream}$), which ranged from 10 $tN.y^{-1}$ (2013-2014) to 98 $tN.y^{-1}$ (2014-2015), with 59 $tN.y^{-1}$ in 2017-2018 (**Fig. 10**). The last part of the stream located in the immediate coastal environment was responsible for 44% (2014-2015) to 56% (2013-2014) of the DIN inputs to the Or lagoon, and 48% in 2017-2018.

The contribution of groundwater to annual DIN inputs at the Salaison outlet estimated with the annual groundwater-driven DIN inputs at the Salaison outlet (i.e. $F_{gw} + \Delta F_{gw}$) and DIN inputs

474 at the Salaison outlet (i.e. $F_{station}+\Delta F_{downstream}$) ranged from 89% (2014-2015) to 94% (2013-
475 2014). Hence, adding the results obtained from the downstream part of the Salaison to the
476 annual DIN inputs increased the overall contribution of groundwater to this perennial stream,
477 making it the main source of DIN in the stream.

5. Discussion

5.1. Uncertainties on the combined methods

5.1.1. Uncertainties on the piezometric contours

Piezometric contours were determined from measurements of the level of well water for one campaign in high flows (**Fig. 3**). The lack of information about aquifer geometry (cross-section) and hydrodynamic parameters (hydraulic transmissivity) did not allow to estimate groundwater flows using Darcy's law (Schilling and Wolter, 2007), but the method nevertheless provides a first qualitative overview of surface water / groundwater interactions around the Salaison River. Indeed, the hydraulic gradients estimated from the piezometric contours confirm the importance of the downstream part of the stream. Groundwater contributions to DIN inputs in the stream were estimated without using the groundwater catchment data, and adding a qualitative overview from a broader scale supports the conclusions of the study on the hydrogeological functioning of the area.

5.1.2. Uncertainties on DIN inputs upstream from the gauging station

Hydrograph separation of high frequency water flow data combined with previous stream data analysis made it possible to assess the contribution of groundwater, and the baseflow results in this study are in agreement with those of a perennial stream (Eckhardt, 2008). Our results highlight the fact that, as the main source of DIN in the stream, groundwater was diluted by a low DIN / low conductivity surface water end-member (**Fig. 5**). Nevertheless, surface driven DIN fluxes can be significant even with low DIN concentrations, especially during flood events where water flow increases significantly. Thus, considering that groundwater contribution at the gauging station was 100% would have led to an overestimation of groundwater loads.

The non-conservative relation of DIN with conductivity upstream from the gauging station suggested that using DIN concentrations in groundwater from 'theoretical' groundwater end-member would have overestimated the DIN flux upstream from the gauging station (**Fig. 5**). The concentrations of DIN measured in the stream at the gauging station represent the combination of DIN inputs and DIN consumption upstream, either during the transit between the aquifer and the stream or during transit along the stream, for example due to uptake by plants or consumption by microorganisms (Cooper, 1990). Indeed, not taking the consumption processes along the stream into account would have led to a 50% overestimation (i.e. from the 'theoretical' end-member 600 $\mu mol.L^{-1}$ to the 'effective' end-members 300 $\mu mol.L^{-1}$). Still, estimating the groundwater driven DIN flux with a constant 'effective' end-member concentration deduced from groundwater samples relies on the assumption that mixing with surface water is conservative. **Figure 5** shows that, in practice, this is not the case, but the 'effective' groundwater end-member provides a more realistic estimation of the contribution of groundwater upstream. Additional data for DIN for conductivity between 800 and 1200 $\mu S.cm^{-1}$ in the stream would enable to reduce the uncertainty of the groundwater end-member (i.e. conductivity associated with the 'effective groundwater end-member') (**Fig. 5**).

5.1.3. Uncertainties on DIN inputs downstream from the gauging station

The absolute uncertainty of groundwater inflow estimated from the radon mass balance ΔQ_{gw} is related to all mass balance parameters, with higher uncertainty for the April and May campaigns (**Fig. 7**). The main parameters which influence uncertainty are the choice of radon

end-member concentrations and disscharge measurements (as initial inputs to the model). Despite their high uncertainties, the model outputs (water flow at the Salaison outlet) are within the same confidence intervals as manual gauging at the outlet. Importantly, the results of this study suggest that all the water that discharged into the downstream part of the river was groundwater driven (direct inflow + canal inputs) (**Fig. 9**). In future studies, differential water flow gauging between the gauging station and the outlet would be sufficient to estimate the additional groundwater flow (for periods with no significant surface flow).

Groundwater inputs downstream from the gauging station estimated in this study were extrapolated to obtain an overall DIN flux at the scale of a hydrological cycle, based on the assumption that the 7-month campaigns were representative of the whole hydrological year. Indeed, the first months of the hydrological cycle 2017-2018 were particularly dry (**Fig. 7**), with 56 mm of rainfall from September to December 2017. Furthermore, the seven campaigns were able to capture different water flows (from 55 $L.s^{-1}$ to 825 $L.s^{-1}$) which are representative of 92% of the hydrological conditions in the stream. Thus, studying water flow and changes in DIN flux in seven campaigns conducted from January to July enabled us to estimate the general interaction processes between the groundwater and the surface water for the whole hydrological cycle (from September to the following August), even though it is difficult to capture the correlation with the behaviour of the aquifer. Sampling campaigns did not capture flood events, but the results of this study show that the relative increase in high flows was not significant (**Fig. 8**). Indeed, water flow and DIN flux were already high at the gauging station and remained stable until the outlet.

5.1.4. Combining methods to understand surface water / groundwater interaction in the Salaison River

In this study, complementary methods were used to improve our understanding of surface water / groundwater interactions along the Salaison River. High frequency water flow and DIN data were available for the upstream part of the Salaison, enabling the use of hydrograph baseflow separation and flow interval classification methods to estimate DIN fluxes. Downstream from the gauging station, a radon mass balance highlighted the predominance of groundwater driven DIN inputs in this part of the stream. Combining the results of the downstream radon mass balance with results of the upstream hydrograph separation results enabled estimation of groundwater-driven DIN fluxes at the Salaison outlet. Combining the methods did not reduce uncertainties, but validated the robustness of the results by approaching the study from different angles (Baudron et al., 2015; Martinez et al., 2015).

5.2. Importance of the downstream part of the Salaison River

This study demonstrated that the majority of DIN fluxes at the Salaison River outlet are groundwater driven (**Fig. 10**). As a perennial stream, groundwater is a major contributor to stream flow and an even more important contributor to DIN as a result of the high DIN concentrations in the aquifer (Adyasari et al., 2018; Exner-Kittridge et al., 2016; Schilling et al., 2018). The downstream part of the Salaison River in particular delivers 44% to 56% of the DIN inputs to the Or lagoon, even though it only covers 25% of the surface watershed. Moreover, inputs of groundwater downstream are less likely to be consumed before arriving at

the Salaison outlet compared with inputs to the upstream part of the stream, since their transit time before reaching the outlet is shorter (Seitzinger, 1988).

In addition, the water in the two canals located downstream from the gauging station originates from groundwater (**Fig. 9**). The original purpose of the two canals was to receive waste water and storm water in high flow conditions (Aquascop, 2013), but they also acted as pathways which enabled groundwater to reach the main channel by improving its drainage contact with the aquifer (Rozemeijer and Broers, 2007). Groundwater is carried to the Salaison river through these outlets, adding flow to the direct groundwater discharge which occurs all along the river. The Roubine canal delivers a significant proportion of the groundwater flow (from 10 to 40 $L.s^{-1}$) to the last part of the Salaison River and the short transit time before reaching Or lagoon limits the consumption of associated DIN fluxes.

Inflows of groundwater to the downstream part of the Salaison River are a major source of DIN and these inputs are not monitored by the gauging station, suggesting that the position of the gauging station may have a significant impact on the estimation of DIN fluxes at the Salaison outlet (**Fig. 10**). Locating the Salaison gauging station 2 000 m downstream, at the limit between alluvial bedrock and lagoon silt would make it possible to monitor water flow and DIN concentrations more accurately while still avoiding the intrusion of lagoon water (**Fig. 3**). The results of this study emphasize the need to understand surface water /groundwater interactions on the continent to satisfactorily monitor nutrient fluxes to the coastal zone (Delconte et al., 2014; Jin et al., 2016). Nevertheless, for the five hydrological cylces studied, annual DIN inputs at the Salaison outlet were found to be correlated with annual rainfall (R^2=0.92; $y = 0.106x - 26$, *data not shown*). Thus, available rainfall data could provide a preliminary estimation of the annual load reaching the Or lagoon, as long as groundwater and surface runoff constitute the main DIN sources in the stream.

5.3. Groundwater is a significant source of DIN in the Or lagoon

The final aim of this study was to estimate total DIN inputs from the alluvial aquifer to the Or lagoon. Previous studies had concluded that no direct submarine groundwater discharge in the lagoon or from other groundwater pathways from the Villafranchien aquifer to the Or lagoon needed to be identified. Since geological characteristics on the northern border of the lagoon at the limit with the aquifer are similar for all the northern streams, our work focused on the Salaison River as a representative area for surface water / groundwater interactions. First, the hydraulic gradients from the piezometric contour of the aquifer around the Salaison river indicated that in high flow conditions, most of the groundwater discharges upstream from the silt layer (**Fig. 3**). A change in permeability must cause groundwater outflow upstream from the alluvium/silt interface (Santamaria, 1995), not only in the Salaison groundwater catchment but also in the surrounding wetlands on the northern part of the lagoon (**Fig. 1a**). In these areas, evaporation and plant uptake are high and man-made embankments often divide up the natural areas, so the real quantity of water that arrives in the lagoon in this way may be negligible. The streams thus represent the only outlets for the water table, with the Salaison River as one of the main streams. Although the Salaison only accounts for 17% of the Or surface watershed, it delivers 59% of total freshwater originating from the northern streams (Colin et al., 2017) and, according to our results, including significant groundwater-driven inputs of DIN (> 90%) (**Fig.**

603 **10**). This study demonstrates that the Salaison River is a major conveyor of groundwater-driven
604 DIN to the Or lagoon, and is probably representative of groundwater inputs to the Or lagoon
605 from other natural streams nearby, owing to similar hydrology and hydrogeology. Moreover,
606 the important aquifer interaction with the stream could explain the important contribution of
607 the Salaison to the freshwater inputs in comparison with its small watershed.

608 To estimate groundwater driven DIN inputs from all these northern streams, two extreme
609 hydrological behaviours can be assumed. First, the Salaison can be considered as the only
610 stream fed by groundwater in the northern part of the watershed. Hence, depending on
611 hydrological conditions, this study suggests that 10 (dry hydrological cycle) to 98 $tN.y^{-1}$ (wet
612 hydrological cycle) originating from the Villafranchien aquifer reach the Or lagoon every year
613 (**Fig. 10**). It can also be assumed that all the northern streams are characterised by similar
614 surface water/groundwater interactions and DIN end-members as those of the Salaison River.
615 Since these stream supply 40% of freshwater to the Or lagoon (Colin et al., 2017), assuming
616 that 90% of this freshwater originates from groundwater, DIN inputs can be estimated. In this
617 case, 17 (dry hydrological cycle) to 163 $tN.y^{-1}$ (wet hydrological cycle) of groundwater driven
618 DIN reach the Or lagoon. Extrapolations to other northern streams involve considerable
619 uncertainties because (1) the surface water in other parts of the aquifer might constitute a
620 significant DIN source depending on land occupation, (2) the groundwater catchment of the
621 Salaison River is larger than the surface watershed, thereby reducing the aquifer system of
622 other streams including their groundwater discharge (**Fig. 3**). Despite these uncertainties, these
623 simple estimations provide an order of magnitude for total groundwater driven DIN inputs to
624 the Or lagoon, with minimum (results for the Salaison only) and maximum values.

625 **5.4. Implications for managements actions in the Or lagoon**

626 This study has shown that, even though groundwater does not discharge directly into the
627 lagoon, groundwater-driven inputs to the inflowing stream are a significant source of DIN to
628 the Or lagoon and are only partially taken into account in current observations made at the
629 gauging stations. Our investigation focussed on DIN, at the origin of eutrophication - with the
630 predominance of nitrate from the Salaison (74% to 99% of total DIN). Similar considerations
631 apply to phosphorus or crop protection products (pesticides), for example, and, depending on
632 concentration in the groundwater and the half-life of the molecule concerned, inputs to the
633 coast may also be significant. This study has shown that the aquifer and its subsurface
634 catchment have to be taken into account in territorial strategies (Adyasari et al., 2018; Stieglitz
635 et al., 2013). This implies that the area targeted by management actions aimed at reducing
636 inputs of the nutrient to the coastal zone has to extend from the watershed to the groundwater
637 catchment. The residence time of water in the aquifer is another important parameter to take
638 into account in management planning and monitoring: if the travel time is long, results of
639 management actions will only be observed with a significant lag time (Fenton et al., 2011; van
640 Lanen and Dijksma, 1999; Vervloet et al., 2018). Concentrations of DIN in the aquifer have
641 remained relatively constant in the past decade, evidence that management actions in the
642 watershed have not improved the quality of the groundwater so far. Groundwater dating should
643 give an indication of time needed to see improvement in the nutrient concentration at the
644 aquifer outlet (Aquilina et al., 2012).

Conclusions

The complementary methods used in this study enabled us to investigate surface water / groundwater interactions in the upstream and downstream sections of the Salaison River. Groundwater was shown to be the main source of DIN (mainly NO_3) contamination of the Salaison River, thereby revealing streams to be indirect pathways for groundwater to reach the Or lagoon. Inputs are naturally governed by hydrogeological conditions and are usually considerably underestimated when they are only measured at the gauging station. The high level of groundwater driven DIN inputs estimated in this study could inhibit restoration of the Or lagoon for many years. The results of the study improve our understanding of indirect groundwater-driven nutrient inputs from an alluvial aquifer to the coastal zone and of the land/sea continuum.

Acknowledgements

This research was funded by the French National Research Agency (ANR) through the ANR @RAction chair of excellence (ANR-14-ACHN-0007-01 - T Stieglitz). This research is part of a PhD projet funded by IFREMER, BRGM and CEREGE. The authors acknowledge A Nefzi, E Bousquet and S Pistre for their support with data collection and analysis. We are grateful to F Maldan (BRGM Montpellier) for all his help in the field, and also to C Saguet and L Dijoux (IFREMER Sète). DIN samples were analysed at IFREMER Sète laboratory (COFRAC - accredited) with the help of M Fortune, E Foucault and G Messiaen. We thank F Colin (SupAgro Montpellier), R De Wit (CNRS Montpellier), E Roque (IFREMER Sète), P Souchu (IFREMER Nantes) and JB Martin (University of Florida) for constructive comments on our paper. We are grateful of the two reviewers that provided useful comments to improve the manuscript.

References

Adyasari, D., Oehler, T., Afiati, N., Moosdorf, N., 2018. Groundwater nutrient inputs into an urbanized tropical estuary system in Indonesia. Sci. Total Environ. 627, 1066–1079. https://doi.org/10.1016/J.SCITOTENV.2018.01.281

Aminot, A., Kerouel, R., 2007. Dosage automatique des nutriments dans les eaux marines : méthodes en flux continu. Editions Ifremer, 188 p.

Aquascop, 2013. Suivi 2012 de la qualité des eaux des bassins versants de l'étang de Thau, de l'étang de l'Or, du Lez et de la Mosson. Aquascop/7197 - 307 p.

Aquilina, L., Vergnaud-Ayraud, V., Labasque, T., Bour, O., Molénat, J., Ruiz, L., de Montety, V., De Ridder, J., Roques, C., Longuevergne, L., 2012. Nitrate dynamics in agricultural catchments deduced from groundwater dating and long-term nitrate monitoring in surface- and groundwaters. Sci. Total Environ. 435–436, 167–178. https://doi.org/10.1016/J.SCITOTENV.2012.06.028

Avery, E., Bibby, R., Visser, A., Esser, B., Moran, J., 2018. Quantification of Groundwater Discharge in a Subalpine Stream Using Radon-222. Water 10, 100 p. https://doi.org/10.3390/w10020100

Banks, E.W., Simmons, C.T., Love, A.J., Shand, P., 2011. Assessing spatial and temporal connectivity between surface water and groundwater in a regional catchment: Implications for regional scale water quantity and quality. J. Hydrol. 404, 30–49. https://doi.org/10.1016/J.JHYDROL.2011.04.017

Basset, A., Elliott, M., West, R.J., Wilson, J.G., 2013. Estuarine and lagoon biodiversity and their natural goods and services. Estuar. Coast. Shelf Sci. 132, 1–4. https://doi.org/10.1016/J.ECSS.2013.05.018

Baudron, P., Cockenpot, S., Lopez-Castejon, F., Radakovitch, O., Gilabert, J., Mayer, A., Garcia-Arostegui, J.L., Martinez-Vicente, D., Leduc, C., Claude, C., 2015. Combining radon, short-lived radium isotopes and hydrodynamic modeling to assess submarine groundwater discharge from an anthropized semiarid watershed to a Mediterranean lagoon (Mar Menor, SE Spain). J. Hydrol. 525, 55–71. https://doi.org/10.1016/j.jhydrol.2015.03.015

Blaise, M., Dorfliger, N., Le Strat, P., Ladouche, B., 2008. Etang de l'Or : relations entre les eaux souterraines de l'aquifère de sub-surface et l'étang de l'Or en liaison avec l'occupation du sol. BRGM/RP-55367-FR - 275 p.

Burnett, W.C., Aggarwal, P.K.K., Aureli, A., Bokuniewicz, H., Cable, J.E.E., Charette, M.A.A., Kontar, E., Krupa, S., Kulkarni, K.M.M., Loveless, A., Moore, W.S.S., Oberdorfer, J.A.A., Oliveira, J., Ozyurt, N., Povinec, P., Privitera, A.M.G.M.G., Rajar, R., Ramessur, R.T.T., Scholten, J., Stieglitz, T., Taniguchi, M., Turner, J.V. V., 2006. Quantifying submarine groundwater discharge in the coastal zone via multiple methods. Sci. Total Environ. 367, 498–543. https://doi.org/10.1016/j.scitotenv.2006.05.009

706 Burnett, W.C., Dulaiova, H., 2003. Estimating the dynamics of groundwater input into the
707 coastal zone via continuous radon-222 measurements. J. Environ. Radioact. 69, 21–35.
708 https://doi.org/10.1016/S0265-931X(03)00084-5

709 Burnett, W.C., Taniguchi, M., Oberdorfer, J., 2001. Measurement and significance of the direct
710 discharge of groundwater into the coastal zone. J. Sea Res. 46, 109–116.
711 https://doi.org/10.1016/S1385-1101(01)00075-2

712 Chapman, T., 1999. A comparison of algorithms for stream flow recession and baseflow
713 separation. Hydrol. Process. 13, 701–714. https://doi.org/10.1002/(SICI)1099-
714 1085(19990415)13:5<701::AID-HYP774>3.0.CO;2-2

715 Charette, M.A., Buesseler, K.O., Andrews, J.E., 2001. Utility of radium isotopes for evaluating
716 the input and transport of groundwater-derived nitrogen to a Cape Cod estuary. Limnol.
717 Oceanogr. 46, 465–470. https://doi.org/10.4319/lo.2001.46.2.0465

718 Cloern, J.E., 2001. Our evolving conceptual model of the coastal eutrophication problem. Mar.
719 Ecol. Prog. Ser. https://doi.org/10.3354/meps210223

720 Colin, F., Crabit, A., Augas, J., Garnier, F., Favre, L., Lilti, V., Verlingue, U., 2017. Apports
721 d'eau aux lagunes côtières méditerranéennes - Propositions méthodologiques pour la
722 quantification des écoulements basées sur des mesures légères et des modèles
723 synthétiques. Rapport de fin de projet Agence de l'Eau RMC. Montpellier SupAgro - 50
724 p.

725 Cook, P.G., Favreau, G., Dighton, J.C., Tickell, S., 2003. Determining natural groundwater
726 influx to a tropical river using radon, chlorofluorocarbons and ionic environmental tracers.
727 J. Hydrol. 277, 74–88. https://doi.org/10.1016/S0022-1694(03)00087-8

728 Cook, P.G., Lamontagne, S., Berhane, D., Clark, J.F., 2006. Quantifying groundwater
729 discharge to Cockburn River, southeastern Australia, using dissolved gas tracers 222 Rn
730 and SF 6. Water Resour. Res. 42. https://doi.org/10.1029/2006WR004921

731 Cook, P.G., Wood, C., White, T., Simmons, C.T., Fass, T., Brunner, P., 2008. Groundwater
732 inflow to a shallow, poorly-mixed wetland estimated from a mass balance of radon. J.
733 Hydrol. 354, 213–226. https://doi.org/10.1016/j.jhydrol.2008.03.016

734 Cooper, A.B., 1990. Nitrate depletion in the riparian zone and stream channel of a small
735 headwater catchment. Hydrobiologia 202, 13–26. https://doi.org/10.1007/BF00027089

736 de Jonge, V.N., Elliott, M., Orive, E., 2002. Causes, historical development, effects and future
737 challenges of a common environmental problem: eutrophication. Hydrobiologia 475/476,
738 1–19. https://doi.org/10.1023/A:1020366418295

739 Delconte, C.A., Sacchi, E., Racchetti, E., Bartoli, M., Mas-Pla, J., Re, V., 2014. Nitrogen inputs
740 to a river course in a heavily impacted watershed: A combined hydrochemical and isotopic
741 evaluation (Oglio River Basin, N Italy). Sci. Total Environ. 466–467, 924–938.
742 https://doi.org/10.1016/J.SCITOTENV.2013.07.092

743 Derolez, V., Fiandrino, A., Munaron, D., 2014. Bilan sur les principales pressions pesant sur

les lagunes méditerranéennes et leurs liens avec l'état DCE. Rapport Ifremer/RST-LER/LR 14-20 - 46 p.

Derolez, V., Gimard, A., Munaron, D., Ouisse, V., Messiaen, G., Fortune, M., Poirrier, S., Mortreux, S., Guillou, J.-L., Brun, M., Provost, C., Hatey, E., Bec, B., Malet, N., Fiandrino, A., 2017. OBSLAG 2016 - volet eutrophisation. Etat DCE des lagunes méditerranéennes (eau et phytoplancton, période 2011-2016). Développement d'indicateurs de tendance et de variabilité. Ifremer/RST/LER/LR/17.10 - 75 p.

Eckhardt, K., 2008. A comparison of baseflow indices, which were calculated with seven different baseflow separation methods. J. Hydrol. 352, 168–173. https://doi.org/10.1016/j.jhydrol.2008.01.005

Eckhardt, K., 2005. How to construct recursive digital filters for baseflow separation. Hydrol. Process. 19, 507–515. https://doi.org/10.1002/hyp.5675

Exner-Kittridge, M., Strauss, P., Blöschl, G., Eder, A., Saracevic, E., Zessner, M., 2016. The seasonal dynamics of the stream sources and input flow paths of water and nitrogen of an Austrian headwater agricultural catchment. Sci. Total Environ. 542, 935–945. https://doi.org/10.1016/J.SCITOTENV.2015.10.151

Fenton, O., Schulte, R.P.O., Jordan, P., Lalor, S.T.J., Richards, K.G., 2011. Time lag: a methodology for the estimation of vertical and horizontal travel and flushing timescales to nitrate threshold concentrations in Irish aquifers. Environ. Sci. Policy 14, 419–431. https://doi.org/10.1016/J.ENVSCI.2011.03.006

Jin, L., Whitehead, P.G., Heppell, C.M., Lansdown, K., Purdie, D.A., Trimmer, M., 2016. Modelling flow and inorganic nitrogen dynamics on the Hampshire Avon: Linking upstream processes to downstream water quality. Sci. Total Environ. 572, 1496–1506. https://doi.org/10.1016/J.SCITOTENV.2016.02.156

Johannes, R., 1980. The Ecological Significance of the Submarine Discharge of Groundwater. Mar. Ecol. Prog. Ser. 3, 365–373. https://doi.org/10.3354/meps003365

Khadka, M.B., Martin, J.B., Kurz, M.J., 2017. Synoptic estimates of diffuse groundwater seepage to a spring-fed karst river at high spatial resolution using an automated radon measurement technique. J. Hydrol. 544, 86–96. https://doi.org/10.1016/J.JHYDROL.2016.11.013

Kjerfve, B., Magill, K.., 1989. Geographic and hydrodynamic characteristics of shallow coastal lagoons. Mar. Geol. 88, 187–199. https://doi.org/10.1016/0025-3227(89)90097-2

Lanini, S., Caballero, Y., Seguin, J.-J., Maréchal, J.-C., 2016. ESPERE-A Multiple-Method Microsoft Excel Application for Estimating Aquifer Recharge. Groundwater 54, 155–156. https://doi.org/10.1111/gwat.12390

Martinez, J.L., Raiber, M., Cox, M.E., 2015. Assessment of groundwater–surface water interaction using long-term hydrochemical data and isotope hydrology: Headwaters of the Condamine River, Southeast Queensland, Australia. Sci. Total Environ. 536, 499–516.

https://doi.org/10.1016/J.SCITOTENV.2015.07.031

Meinesz, C., Derolez, V., Bouchoucha, M., 2013. Base de données « pressions sur les lagunes méditerranéennes ». Analyse des liens état – pression, Rapport Ifremer RST.ODE/LER-PAC/13-11 - 71 p.

Menció, A., Galán, M., Boix, D., Mas-Pla, J., 2014. Analysis of stream–aquifer relationships: A comparison between mass balance and Darcy's law approaches. J. Hydrol. 517, 157–172. https://doi.org/10.1016/J.JHYDROL.2014.05.039

Mooney, H., Larigauderie, A., Cesario, M., Elmquist, T., Hoegh-Guldberg, O., Lavorel, S., Mace, G.M., Palmer, M., Scholes, R., Yahara, T., 2009. Biodiversity, climate change, and ecosystem services. Curr. Opin. Environ. Sustain. 1, 46–54. https://doi.org/10.1016/J.COSUST.2009.07.006

Moore, W.S., 2010. The Effect of Submarine Groundwater Discharge on the Ocean. Ann. Rev. Mar. Sci. 2, 59–88. https://doi.org/10.1146/annurev-marine-120308-081019

Mullinger, N.J., Binley, A.M., Pates, J.M., Crook, N.P., 2007. Radon in Chalk streams: Spatial and temporal variation of groundwater sources in the Pang and Lambourn catchments, UK. J. Hydrol. 339, 172–182. https://doi.org/10.1016/J.JHYDROL.2007.03.010

Newton, A., Brito, A.C., Icely, J.D., Derolez, V., Clara, I., Angus, S., Schernewski, G., Inácio, M., Lillebø, A.I., Sousa, A.I., Béjaoui, B., Solidoro, C., Tosic, M., Cañedo-Argüelles, M., Yamamuro, M., Reizopoulou, S., Tseng, H.-C., Canu, D., Roselli, L., Maanan, M., Cristina, S., Ruiz-Fernández, A.C., Lima, R.F. de, Kjerfve, B., Rubio-Cisneros, N., Pérez-Ruzafa, A., Marcos, C., Pastres, R., Pranovi, F., Snoussi, M., Turpie, J., Tuchkovenko, Y., Dyack, B., Brookes, J., Povilanskas, R., Khokhlov, V., 2018. Assessing, quantifying and valuing the ecosystem services of coastal lagoons. J. Nat. Conserv. 44, 50–65. https://doi.org/10.1016/J.JNC.2018.02.009

Newton, A., Icely, J., Cristina, S., Brito, A., Cardoso, A.C., Colijn, F., Riva, S.D., Gertz, F., Hansen, J.W., Holmer, M., Ivanova, K., Leppäkoski, E., Canu, D.M., Mocenni, C., Mudge, S., Murray, N., Pejrup, M., Razinkovas, A., Reizopoulou, S., Pérez-Ruzafa, A., Schernewski, G., Schubert, H., Carr, L., Solidoro, C., PierluigiViaroli, Zaldívar, J.-M., 2014. An overview of ecological status, vulnerability and future perspectives of European large shallow, semi-enclosed coastal systems, lagoons and transitional waters. Estuar. Coast. Shelf Sci. 140, 95–122. https://doi.org/10.1016/J.ECSS.2013.05.023

Peterson, R.N., Santos, I.R., Burnett, W.C., 2010. Evaluating groundwater discharge to tidal rivers based on a Rn-222 time-series approach. Estuar. Coast. Shelf Sci. 86, 165–178. https://doi.org/10.1016/J.ECSS.2009.10.022

Quintana, X.D., Moreno-Amich, R., Comín, F.A., 1998. Nutrient and plankton dynamics in a Mediterranean salt marsh dominated by incidents of flooding. Part 1: Differential confinement of nutrients. J. Plankton Res. 20, 2089–2107. https://doi.org/10.1093/plankt/20.11.2089

Rimmelin, P., Dumon, J.-C., Maneux, E., Gonçalves, A., 1998. Study of Annual and Seasonal

821 Dissolved Inorganic Nitrogen Inputs into the Arcachon Lagoon, Atlantic Coast (France).
822 Estuar. Coast. Shelf Sci. 47, 649–659. https://doi.org/10.1006/ECSS.1998.0384

823 Rodellas, V., Garcia-Orellana, J., Masqué, P., Feldman, M., Weinstein, Y., 2015. Submarine
824 groundwater discharge as a major source of nutrients to the Mediterranean Sea. Proc. Natl.
825 Acad. Sci. U. S. A. 112, 3926–30. https://doi.org/10.1073/pnas.1419049112

826 Rodellas, V., Stieglitz, T.C., Andrisoa, A., Cook, P.G., Raimbault, P., Tamborski, J.J., van
827 Beek, P., Radakovitch, O., 2018. Groundwater-driven nutrient inputs to coastal lagoons:
828 The relevance of lagoon water recirculation as a conveyor of dissolved nutrients. Sci.
829 Total Environ. 642, 764–780. https://doi.org/10.1016/J.SCITOTENV.2018.06.095

830 Rozemeijer, J.C., Broers, H.P., 2007. The groundwater contribution to surface water
831 contamination in a region with intensive agricultural land use (Noord-Brabant, The
832 Netherlands). Environ. Pollut. 148, 695–706.
833 https://doi.org/10.1016/J.ENVPOL.2007.01.028

834 Santamaria, L., 1995. Etude preliminaire des transferts d'eau et de solutés à l'étang de l'Or, au
835 travers des formations villafranchiennes dans la plaine de Mauguio-Lunel, interface
836 nappe-étang. Université Montpellier II/ Mémoire de fin d'études - 46 p.

837 Santos, I.R., Peterson, R.N., Eyre, B.D., Burnett, W.C., 2010. Significant lateral inputs of fresh
838 groundwater into a stratified tropical estuary: Evidence from radon and radium isotopes.
839 Mar. Chem. 121, 37–48. https://doi.org/10.1016/J.MARCHEM.2010.03.003

840 Schilling, K.E., Streeter, M.T., Bettis, E.A., Wilson, C.G., Papanicolaou, A.N., 2018.
841 Groundwater monitoring at the watershed scale: An evaluation of recharge and nonpoint
842 source pollutant loading in the Clear Creek Watershed, Iowa. Hydrol. Process. 32, 562–
843 575. https://doi.org/10.1002/hyp.11440

844 Schilling, K.E., Wolter, C.F., 2007. A GIS-based groundwater travel time model to evaluate
845 stream nitrate concentration reductions from land use change. Environ. Geol. 53, 433–
846 443. https://doi.org/10.1007/s00254-007-0659-0

847 Schilling, K.E., Wolter, C.F., 2001. Contribution of Base Flow to Nonpoint Source Pollution
848 Loads in an Agricultural Watershed. Ground Water 39, 49–58.
849 https://doi.org/10.1111/j.1745-6584.2001.tb00350.x

850 Seitzinger, S.P., 1988. Denitrification in freshwater and coastal marine ecosystems: Ecological
851 and geochemical significance. Limnol. Oceanogr. 33, 702–724.
852 https://doi.org/10.4319/lo.1988.33.4part2.0702

853 Slomp, C.P., Van Cappellen, P., 2004. Nutrient inputs to the coastal ocean through submarine
854 groundwater discharge: controls and potential impact. J. Hydrol. 295, 64–86.
855 https://doi.org/10.1016/j.jhydrol.2004.02.018

856 Souchu, P., Bec, B., Smith, V.H., Laugier, T., Fiandrino, A., Benau, L., Orsoni, V., Collos, Y.,
857 Vaquer, A., 2010. Patterns in nutrient limitation and chlorophyll a along an anthropogenic
858 eutrophication gradient in French Mediterranean coastal lagoons. Can. J. Fish. Aquat. Sci.

67, 743–753. https://doi.org/10.1139/F10-018

Stieglitz, T.C., van Beek, P., Souhaut, M., Cook, P.G., 2013. Karstic groundwater discharge and seawater recirculation through sediments in shallow coastal Mediterranean lagoons, determined from water, salt and radon budgets. Mar. Chem. 156, 73–84. https://doi.org/10.1016/j.marchem.2013.05.005

Symbo, 2017. Tableau de bord de suivi environnemental du contrat de bassin de l'Or. OUTIL TECHNIQUE TBSE – Or 2017 - 33 p.

Symbo, 2014. Le Salaison, état des lieux et programme pluriannuel de gestion et de restauration. 30 p.

Taylor, D., Nixon, S., Granger, S., Buckley, B., 1995. Nutrient limitation and the eutrophication of coastal lagoons. Mar. Ecol. Prog. Ser. 127, 235–244. https://doi.org/10.3354/meps127235

van Lanen, H.A.J., Dijksma, R., 1999. Water flow and nitrate transport to a groundwater-fed stream in the Belgian-Dutch chalk region. Hydrol. Process. 13, 295–307. https://doi.org/10.1002/(SICI)1099-1085(19990228)13:3<295::AID-HYP739>3.0.CO;2-O

Vervloet, L.S.C., Binning, P.J., Børgesen, C.D., Højberg, A.L., 2018. Delay in catchment nitrogen load to streams following restrictions on fertilizer application. Sci. Total Environ. 627, 1154–1166. https://doi.org/10.1016/J.SCITOTENV.2018.01.255

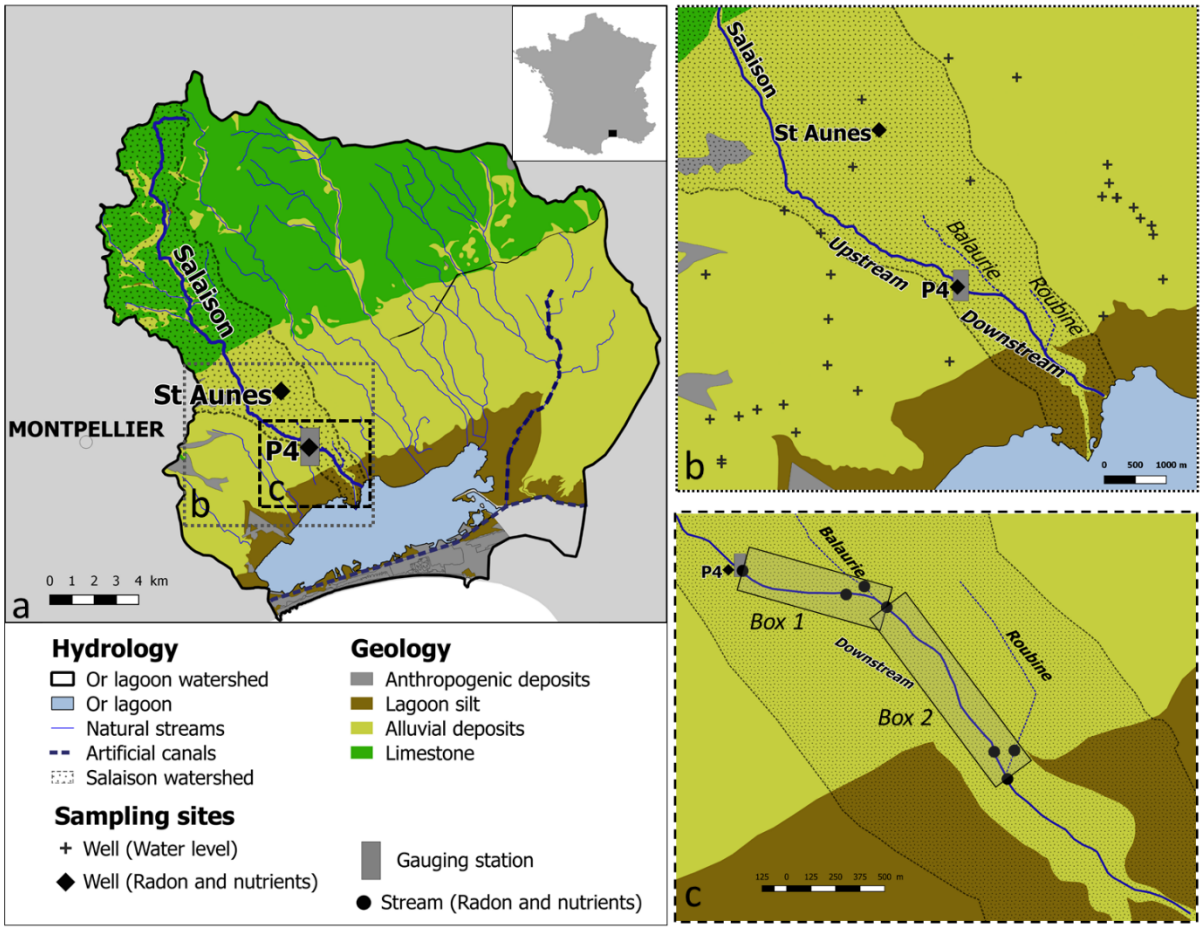


Figure 1: a) Hydrogeological settings and localisation of piezometers for the study site; b) Sampling stations for the piezometric map (water levelled wells) and localisation of the gauging station in Salaison river; c) Sampling sites for the radon sampling downstream of the gauging station and the two associated box models for the radon mass balance.

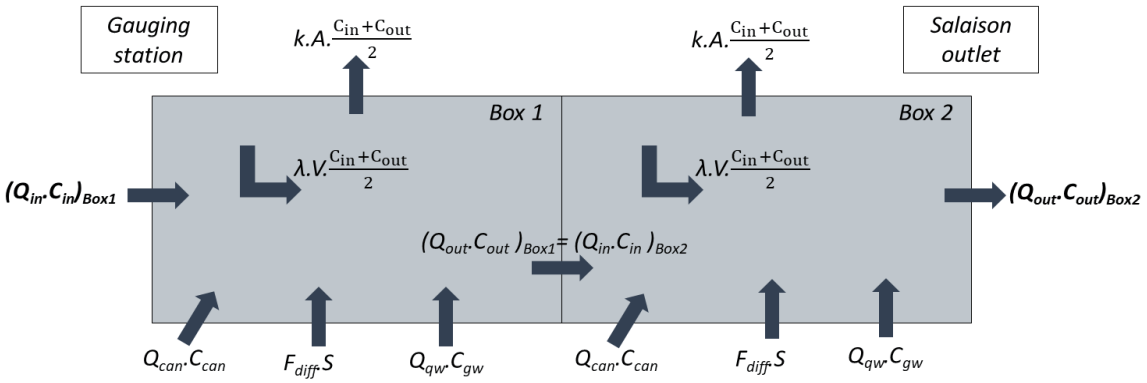


Figure 2: Conceptual scheme of the connected boxes for the radon mass balance in the downstream part of Salaison River: sinks and sources of radon flux ($Bq.s^{-1}$)

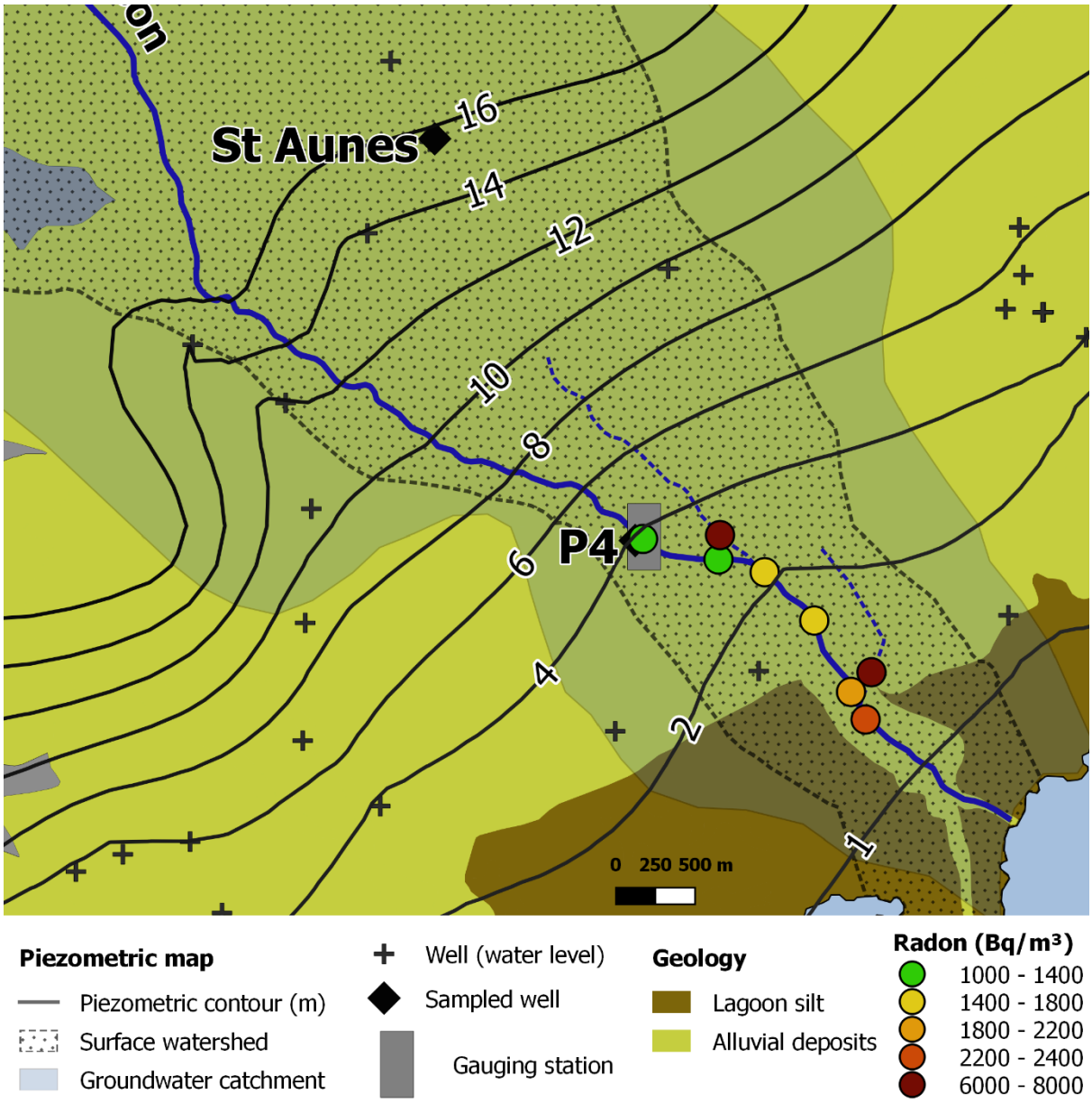


Figure 3: Piezometric maps describing Salaison's groundwater catchment. Salaison watershed is displayed for comparison with the groundwater catchment. On the downstream part of Salaison River, an example of radon concentrations measured on 2/15/2018 is presented, showing significant radon increase due to significant groundwater input downstream.

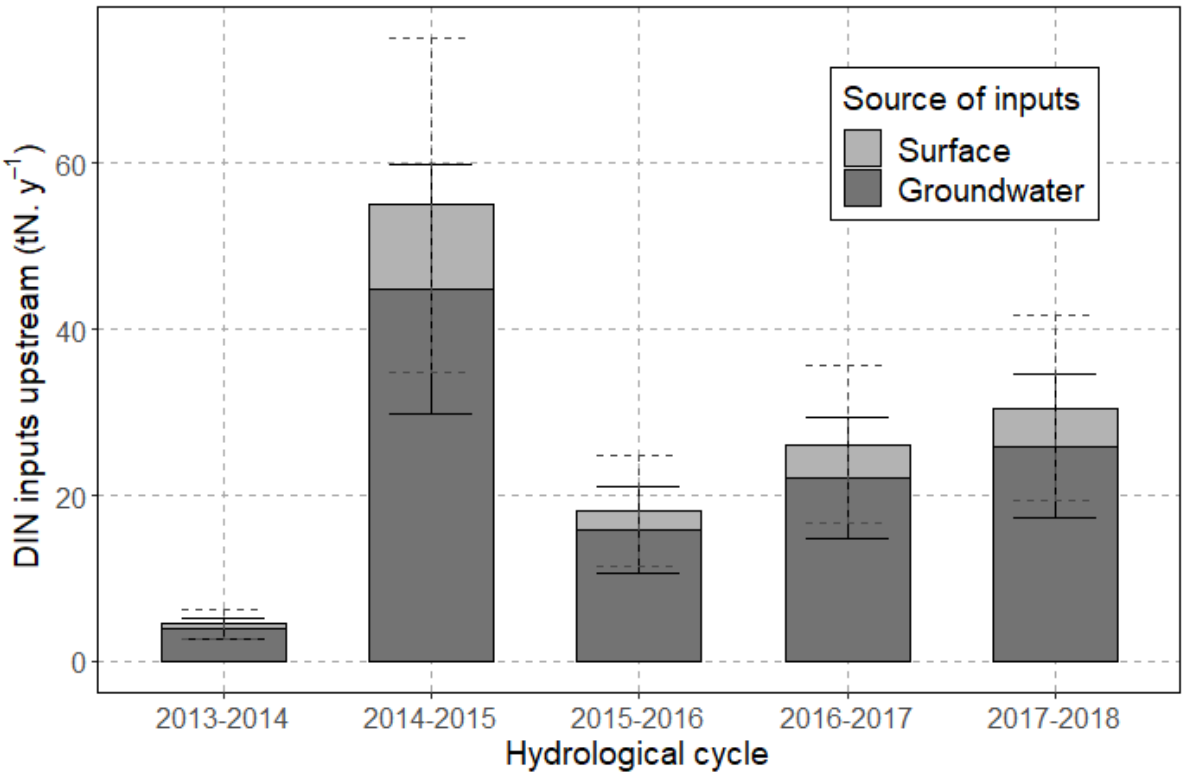


Figure 4: DIN inputs at the gauging station assessed from the flow interval method with data from Salaison gauging station monitoring (combining all sources), and groundwater contribution to the total DIN inputs estimated from baseflow separation and end-member mixing analysis (dark grey).

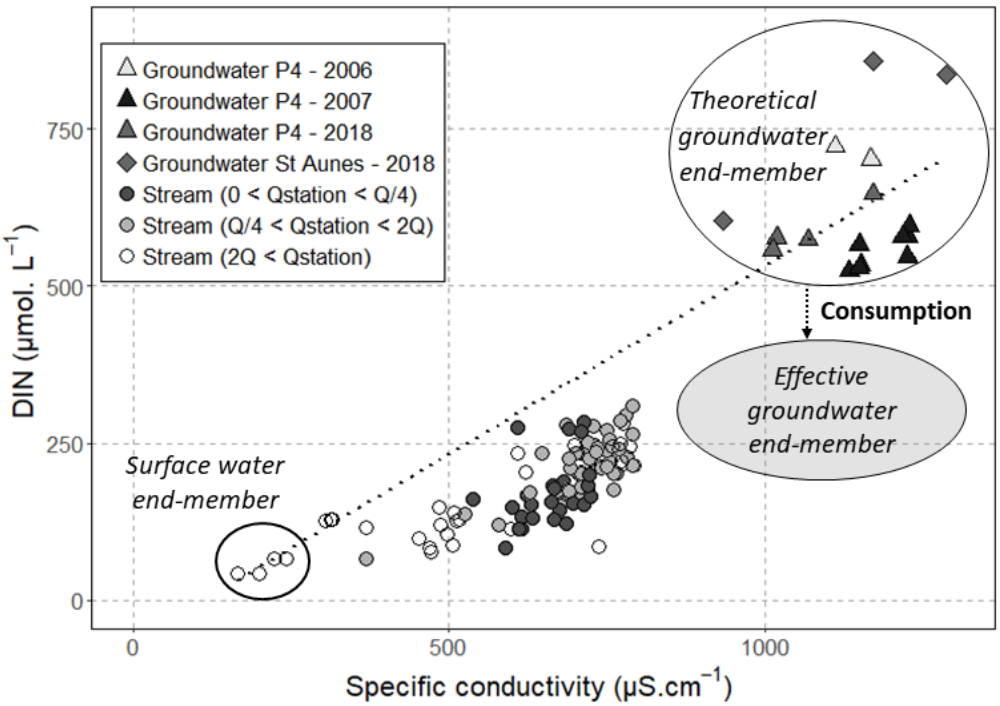


Figure 5: DIN evolution (µmol·L^{-1}) according to specific conductivity (µS·cm^{-1}) measured at Salaison gauging station from 2013 to 2018 (circles) for different water flow classes (in L·s^{-1}) (detailed in Table 2), and in the piezometer P4 in 2006, 2007 and 2018 (triangle) and in the piezometer St Aunes in 2018 (diamond). Dotted black line represents the hypothetical conservative mixing line between high conductivity/high DIN end-member and low conductivity/low DIN end-member.

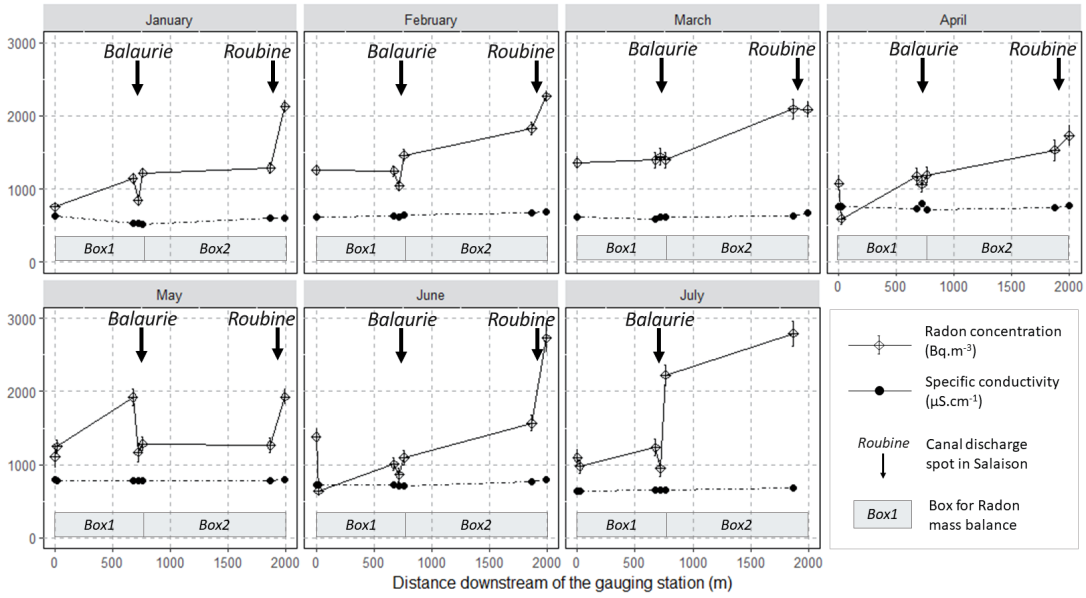


Figure 6: Radon concentration ($Bq.m^{-3}$) and specific conductivity ($\mu S.cm^{-1}$) in the downstream part of the river measured during each campaign in 2018. Grey boxes show the extent of radon mass balance implemented.

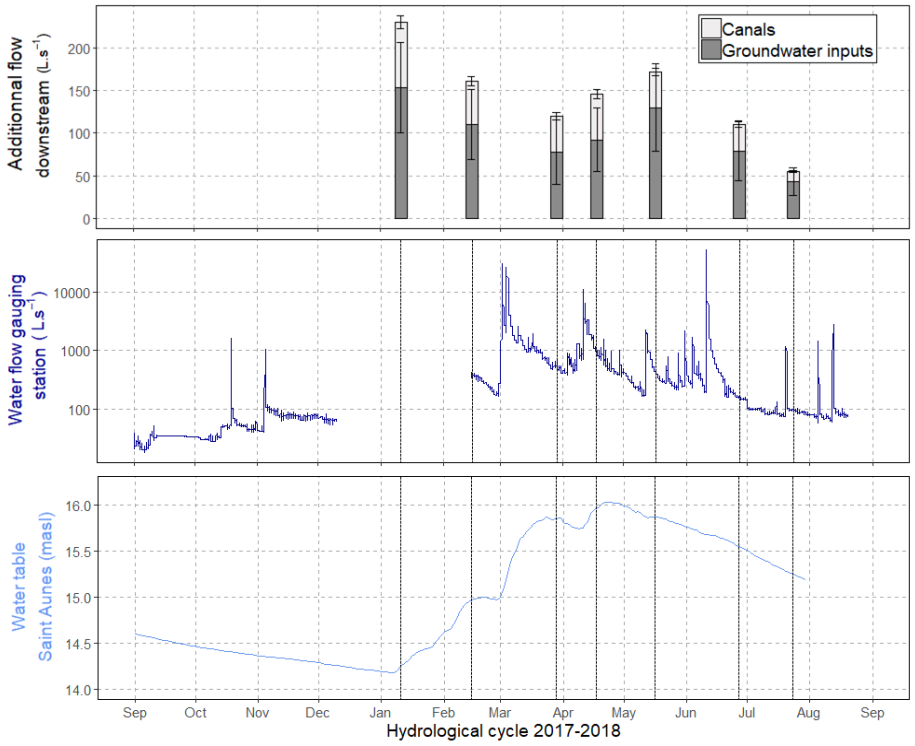


Figure 7: Groundwater discharge in the downstream part of Salaison River ($L.s^{-1}$) assessed with the radon mass balance in 2018 (top); water flow at Salaison gauging station ($L.s^{-1}$) (middle); water table fluctuation (m) at Saint Aunes piezometer (bottom). Vertical lines show campaign periods.

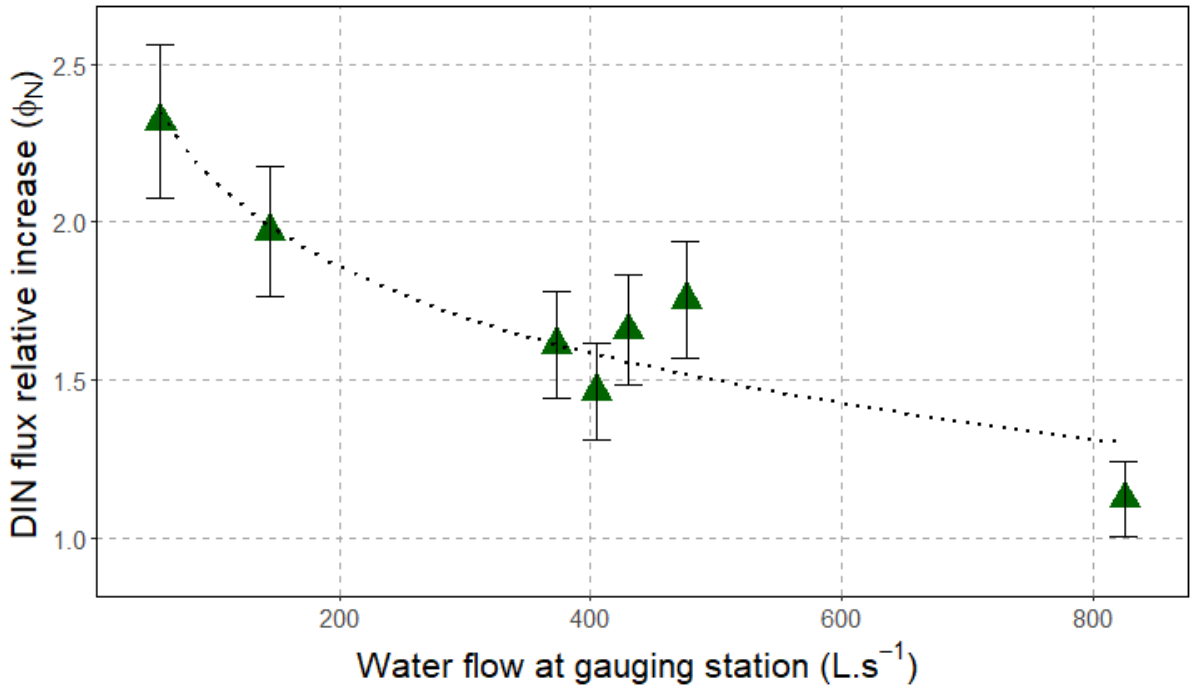


Figure 8: Increase factor of DIN flux downstream from the gauging station according to hydrological conditions at the gauging station (L.s^{-1}).

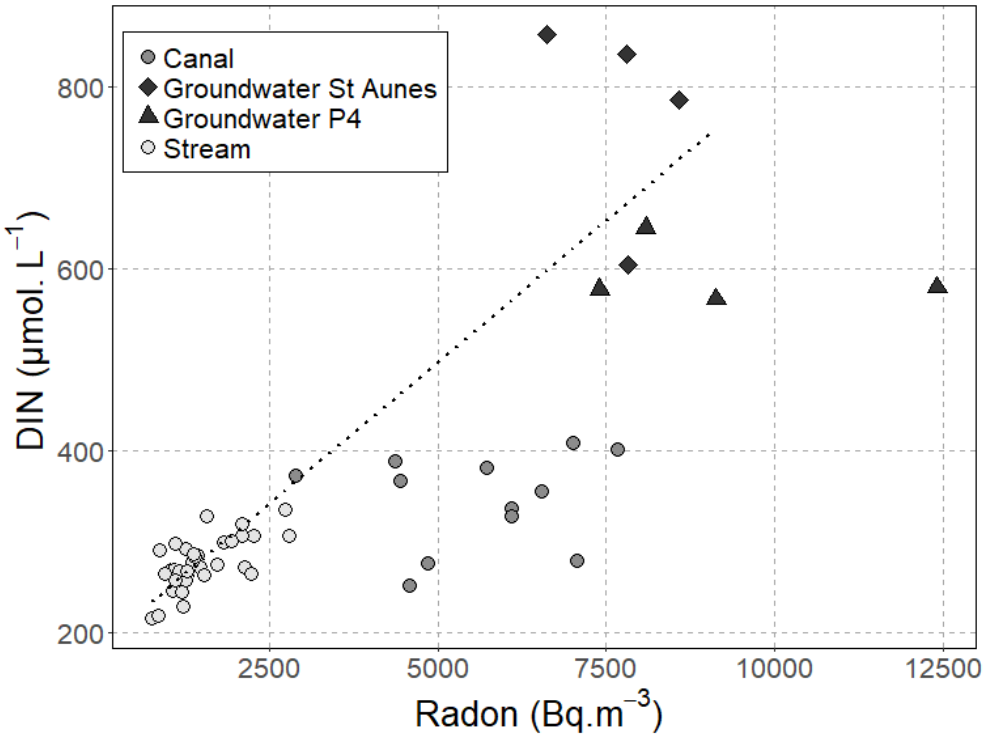


Figure 9: DIN concentrations (µmol.L^{-1}) according to radon concentration (Bq.m^{3}) in the downstream part of Salaison river measured during each campaign in 2018 in the stream (filled circles), in the two canals (hollow circles) and in piezometer P4 (diamonds).

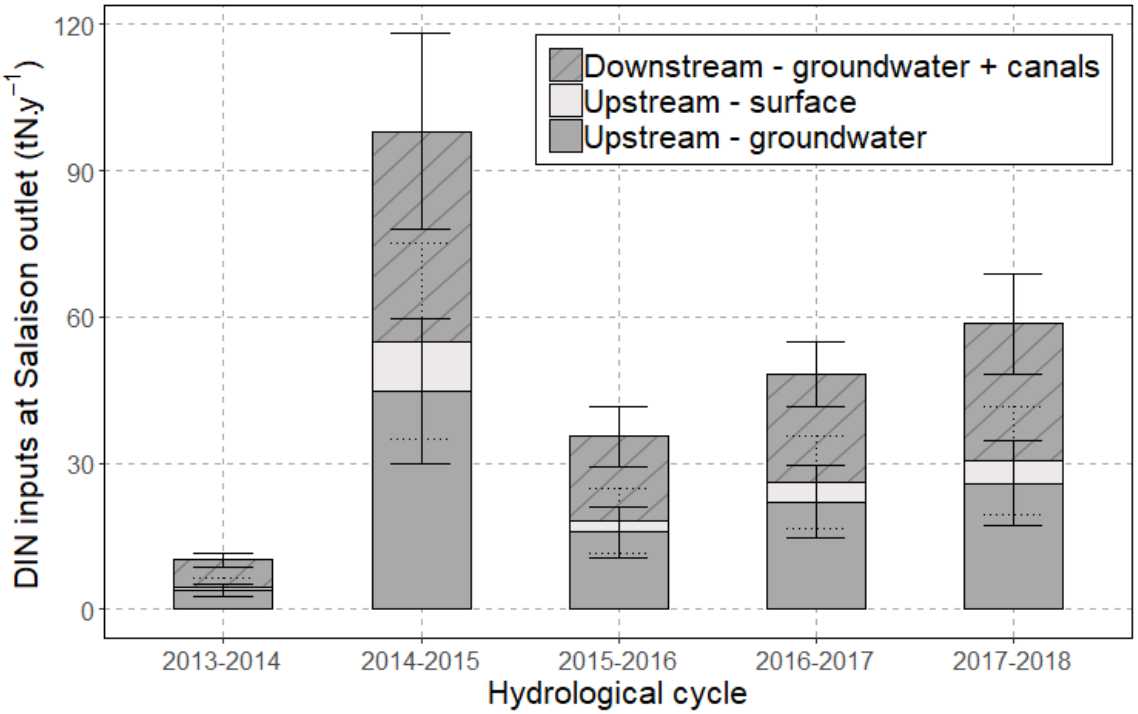


Figure 10: Estimation of DIN inputs to Or lagoon at Salaison outlet: upstream inputs estimated at the gauging station integrating groundwater-driven DIN inputs (dark grey) and surface-driven DIN inputs (light grey); additional groundwater-driven DIN inputs discharging downstream of the gauging station in the river and through the canals (dark grey with oblique lines).

		Upstream	Downstream
Total DIN flux	Waterflow	Data available at the gauging station from 2013 to 2018 - $\mathbf{Q_{station}}$	Radon mass balance – $\mathbf{\Delta Q_{downstream}}$ (Table 3, fig. 6 and 7)
	DIN concentration	Data available at the gauging station from 2013 to 2018 – $\mathbf{[N]_{station}}$ (Fig 5)	Field sampling (Fig 9)
Groundwater driven DIN flux	Groundwater flow	Baseflow separation - $\mathbf{Q_{gw}}$	Radon mass balance - $\mathbf{\Delta Q_{gw}}$ (Table 3, fig. 6 and 7)
	DIN groundwater end-member	Conductivity/DIN correlation– $\mathbf{[N]_{gw_s}}$ (Fig 5)	Radon/DIN correlation – $\mathbf{[N]_{gw_d}}$ (Fig 9)

Table 1: Review of the different methods implemented to study DIN inputs in Salaison River. For each variable, the table presents the origin of the data, the variable name in the study (in bold) and the associated figures showing the data.

Water flow class	**Average DIN ($[N]_{station}$) ($\mu mol.L^{-1}$)**	**Standard deviation ($\mu mol.L^{-1}$)**
$0 < Q_{station} < Q/4$	$\mu = 170$	$\sigma = 62$
$Q/4 < Q_{station} < 2Q$	$\mu = 220$	$\sigma = 64$
$2Q < Q_{station}$	$\mu = 110$	$\sigma = 59$

Table 2: Flow classes and associated average DIN concentrations (source: DREAL) to estimate total nitrogen flux on the upstream part of Salaison river. Classes for each high-frequency water flow ($Q_{station}$) were determined according to average water flow Q (386 $L.s^{-1}$) at the gauging station.

			January		February		March		April		May		June		July	
			Box 1	Box 2	Box 1	Box 2	Box 1	Box 2	Box 1	Box 2	Box 1	Box 2	Box 1	Box 2	Box 1	Box 2
Radon sources	Inflow upstream	Water flow **Qin** ($L.s^{-1}$)	476	529	430	480	405	425	825	854	371	408	145	155	58	87
		Radon concentration **Cin** ($Bq.m^{-3}$)	756	1217	1255	1463	1354	1393	1075	1190	1107	1285	1378	1096	1095	2224
	Inflow from canal	Water flow **Qcan** ($L.s^{-1}$)	19	58	12	39	10	32	12	42	9	31	12	19	12	-
		Radon concentration **Ccan** ($Bq.m^{-3}$)	4842	4358	6545	7665	6095	7016	4842	4358	6094	2883	4569	4441	2299	-
	Diffusion from sediments	Diffusion flux **Fdiff** ($Bq.m^{2}.s^{-1}$)	6,9E-03	6,9E-03	6,9E-03	6,9E-03	6,9E-03	6,9E-03	6,9E-03	6,9E-03	6,9E-03	6,9E-03	6,9E-03	6,9E-03	6,9E-03	6,9E-03
		Sediment surface **S** (m^2)	5410	11888	6705	12093	5182	12093	6553	12217	6401	12093	5029	11229	5029	6205
	Inflow from groundwater	Water flow **Qgw** ($L.s^{-1}$)	model output													
		Radon concentration **Cgw** ($Bq.m^{-3}$)	8087	8087	8087	8087	9132	9132	9132	9132	9158	9158	10212	10212	12411	12411
Radon sinks	Decay	Decay constant **λ** (s^{-1})	2,1E-06	2,1E-06	2,1E-06	2,1E-06	2,1E-06	2,1E-06	2,1E-06	2,1E-06	2,1E-06	2,1E-06	2,1E-06	2,1E-06	2,1E-06	2,1E-06
		Box water volume **V** (m^3)	2324	8699	3227	8884	2389	8885	3383	9378	5819	8885	1955	5430	1955	2742
		Average Radon concentration ($Bq.m^{-3}$)	987	1671	1359	1864	1374	1741	1133	1460	1196	1606	1237	1913	1660	2509
	Atmospheric evasion	Evasion coefficient **k** ($m.s^{-1}$)	2,5E-05	2,5E-05	1,6E-05	1,6E-05	2,3E-05	2,3E-05	1,9E-05	1,9E-05	2,5E-05	2,5E-05	1,9E-05	1,9E-05	1,9E-05	1,9E-05
		Water surface **A** (m^2)	4648	9666	5867	9872	4343	9872	5638	9872	5639	9872	4343	9872	4343	4986
		Average Radon concentration ($Bq.m^{-3}$)	987	1671	1359	1864	1374	1741	1133	1460	1196	1606	1237	1913	1660	2509
	Outflow downstream	Water flow Qout ($L.s^{-1}$)	model output													
		Radon concentration **Cout** ($Bq.m^{-3}$)	1217	2124	1463	2264	1393	2088	1190	1729	1285	1927	1096	2730	2224	2793
Radon mass balance outputs		**Water flowing out Qout ($L.s^{-1}$)**	**529**	**654**	**480**	**591**	**425**	**526**	**854**	**971**	**408**	**545**	**155**	**255**	**87**	**113**
		Groundwater discharge Qgw ($L.s^{-1}$)	**34**	**119**	**38**	**73**	**10**	**69**	**17**	**76**	**26**	**106**	**-2**	**80**	**17**	**26**

Table 3: Sources and sinks of the radon mass balance used in each campaign of this study. Water inflow in box 1 presented here corresponds to the manual measurements at the gauging station; diffusion from sediment was estimated in one sampling and the same value were applied in each

campaign; atmospheric evasion was evaluated at each campaign; groundwater radon concentrations corresponds to the nearest radon measurements made in P4 piezometer.